Journal of Solid State Chemistry 182 (2009) 574–579

Contents lists available at ScienceDirect

Journal of Solid State Chemistry

journal homepage: www.elsevier.com/locate/jssc

A 3D porous zinc MOF constructed from a flexible tripodal ligand: Synthesis, structure, and photoluminescence property

Lili Wen [a], Dong'e Wang [a], Chenggang Wang [a], Feng Wang [a], Dongfeng Li [a,*,1], Kejian Deng [b,*]

[a] Key Laboratory of Pesticide & Chemical Biology of Ministry of Education, College of Chemistry, Central China Normal University, Wuhan 430079, PR China
[b] Key Laboratory of Catalysis and Materials Science of the State Ethnic Affairs Commission & Ministry of Education, South-Central University for Nationalities, Wuhan 430074, PR China

ARTICLE INFO

Article history:
Received 9 September 2008
Received in revised form
18 November 2008
Accepted 24 November 2008
Available online 6 December 2008

Keywords:
Flexible tripodal ligand
Porous MOF
X-ray structure
Zinc(II)

ABSTRACT

A new metal-organic framework, $[Zn_5(trencba)_2(OH)_2Cl_2 \cdot 4H_2O]$ (**1**) [H_3trencba = *N*,*N*,*N*′,*N*′,*N*″,*N*″-tris[(4-carboxylate-2-yl)methyl]-tris(2-aminoethyl)amine], constructed from a flexible tripodal ligand based on C_3 symmetric tris(2-aminoethyl)amine, has been synthesized hydrothermally and characterized by elemental analysis, IR, TG, XRD and single-crystal X-ray diffraction analysis. Compound **1** contains an unprecedented linear penta-nuclear zinc cluster fragment. Each ligand links four penta-nuclear fragments, and every fragment links eight ligands to generate a three-dimensional non-interpenetrated porous framework. The uncoordinated water molecules were observed trapped in the void pores. Compound **1** represents the first example of (6,8)-connected 3D bi-nodal framework based on a single kind of organic ligand. The photoluminescence measurements showed that complex **1** exhibits relatively stronger blue emissions at room temperature than that of the ligand.

1. Introduction

In recent years, the rational design of metal-organic frameworks (MOFs) have attracted great interest [1], and considerable efforts have been focused on the design, synthesis and characterization of new multidimensional MOFs, due to their intriguing variety of architectures and topologies, as well as their tremendous potential applications [2–5]. To date, a variety of uninodal and mixed-connected network topologies have been realized. However, the (6,8)-connected framework is much difficult to achieve because it contains two kinds of high-connected nodes. To the best of our knowledge, only one example of this net had been observed in MOFs constructed from mixed organic ligands to date [6]. Currently, most studies have so far been focused on the assembly of porous MOFs from rigid ligands [7–13]. Unfortunately, multidentate flexible linkers remain rare in the construction of porous MOFs, possibly because of less predictability and difficulty in analyzing the topologies of the coordination architectures [14–20]. In contrast to the rigid ligands, the conformation of flexible ones is variable. Thus, they can meet the coordination geometrical requirement of metal ions through changing their conformation, which may provide more possibility for the construction of unprecedented high-connected frameworks.

Recently, we focus our attentions on the construction, structures and properties of MOFs using flexible tripodal ligand *N*,*N*,*N*′,*N*′,*N*″,*N*″-tris[(4-carboxylate-2-yl)methyl]-tris(2-aminoethyl) amine (H_3trencba), which is obtained from C_3 symmetric tris (2-aminoethyl)amine (tren) and 4-carboxybenzaldehyde. The ligand H_3trencba exhibits two important features: (i) it is a bi-functional ligand possessing both amide and carboxylate moieties, in which three benzoic acids building blocks are connected by a tren spacer. The two different organic functionalities may induce dissymmetric building blocks by coordinating to different metal centers or metal clusters with distinct coordination atoms (N and O), which benefits the formation of mix-connected frameworks; (ii) the carboxylate functionality potentially exhibits rich coordination chemistry and may facilitate core aggregation and it could link discrete clusters into an porous framework because of its bridging ability. Therefore, with the aim of understanding the coordination chemistry of the flexible tripodal ligand, preparing materials with beautiful architecture and excellent physical properties, we start to elaborate new high-dimensional MOFs constructed from H_3trencba. In the present paper, we report the synthesis, structural characterization, and photoluminescence property of a new three-dimensional (3D) porous MOF $[Zn_5(trencba)_2(OH)_2Cl_2 \cdot 4H_2O]$ (**1**). Notably, compound **1** represents the first example of (6,8)-connected 3D bi-nodal framework based on single kind of organic ligand, which contains an unprecedented linear penta-nuclear zinc cluster fragment.

* Corresponding authors.
E-mail addresses: dengkj@scuec.edu.cn (D. Li), dfli@mail.ccnu.edu.cn (K. Deng).
[1] Fax: +86 27 67867232.

0022-4596/$ - see front matter © 2008 Elsevier Inc. All rights reserved.
doi:10.1016/j.jssc.2008.11.031

2. Experimental

The reagents and solvents employed were commercially available and used as received without further purification. The C, H, and N microanalyses were carried out with a Perkin-Elmer 240 elemental analyzer. The IR spectra were recorded on KBr discs on a Bruker Vector 22 spectrophotometer in the 4000–400 cm^{-1} region. NMR spectrum was recorded on a Varian Mercury 400 spectrometer and resonances (δ) are given in parts per million relative to tetramethylsilane. Thermogravimetric analysis was performed on a simultaneous SDT 2960 thermal analyzer. Powder sample of complex **1** was heated from room temperature to 800 °C under flowing N_2 at a heating rate of 10 °C/min. Powder X-ray diffraction patterns were recorded on a RigakuD/max-RA rotating anode X-ray diffractometer with graphite monochromatic Cu$K\alpha$ ($\lambda = 1.542$ Å) radiation at room temperature. Luminescence spectra for the solid samples were recorded with a Hitachi 850 fluorescence spectrophotometer.

2.1. Preparation of H_3trencba · HCl

To a solution of 4-carboxybenzaldehyde (1.35 g, 9 mmol) in 20 mL of CH_3CN was added tren (0.44 g, 3 mmol) in CH_3CN (5 mL). The mixture was refluxed overnight and then the solvent was removed by vacuum evaporation. The intermediate Schiff base was dissolved in CH_3OH (20 mL) and excess $NaBH_4$ (2.27 g, 60 mmol) was added in portions with gentle stirring prior to cooling in an ice bath. After 2 h, the CH_3OH solution was removed to obtain the reduced Schiff base, which was poured into water and then was carefully adjusted to pH = 4–5 with concentrated HCl. After left to stand for 1 h, the resulting white precipitation was filtered off, washed with MeOH and Et_2O. Anal. Calcd for H_3trencba · HCl ($C_{30}H_{37}N_4O_6Cl$): C 61.58, H 6.37, N 9.58; found: C 61.55, H 6.41, N 9.54. IR (KBr, cm^{-1}): 3448(s), 1715(s), 1675(s), 1615(m), 1580(m), 1513(w), 1451(m), 1422(s), 1316(m), 1248(m), 1211(m), 1182(m), 1107(m), 1073(w), 1040(w), 1020(w), 985(m), 917(m), 857(m), 803(m), 773(s), 740(m), 703(m), 623(m), 578(w), 527(w), 427(w). 1H NMR (D_2O, 400 MHz, 298 K): $\delta = 2.35$ (s, 12H, NCH_2CH_2N), 3.49 (s, 6H, CH_2), 7.14 (d, 12H, ph), 7.67 (d, 12H, ph).

2.2. Preparation of $[Zn_5(trencba)_2(OH)_2Cl_2 \cdot 4H_2O]$ **1**

Teflon-lined Parr bombs containing a mixture of H_3trencba · HCl (0.0585 g, 0.1 mmol), $Zn(NO_3)_2 \cdot 6H_2O$ (0.0300 g, 0.1 mmol), NaOH (0.012 g, 0.3 mmol), and water (2 mL), were placed inside an oven at 120 °C. The colorless plate-like crystals for **1** were obtained after 72 h of heating (yield: 51% based on Zn). Calcd for $C_{60}H_{76}Cl_2N_8O_{18}Zn_5$: C, 45.18; H, 4.80; N, 7.02. Found: C, 45.12; H, 4.85; N, 7.05. IR (KBr, cm^{-1}): 3406(m), 1592(s), 1545(s), 1528(m), 1509(w), 1459(w), 1407(vs), 1385(s), 1261(w), 1213(w), 1183(w), 1171(w), 1082(w), 998(m), 961(m), 866(m), 814(m), 776(s), 744(w), 711(m), 651(m), 600(m), 552(w), 523(w), 430(w).

2.3. X-ray crystal structure determinations

Intensities of complex **1** were collected on a Siemens SMART-CCD diffractometer with graphite-monochromatic Mo$K\alpha$ radiation ($\lambda = 0.71073$ Å) using the SMART and SAINT programs [21]. The structures were solved by direct methods and refined on F^2 using full-matrix least-squares methods with SHELXTL version 5.1 [22]. Anisotropic thermal parameters were refined for the non-hydrogen atoms. Crystallographic data and other pertinent information for **1** are summarized in Table 1. Selected bond lengths and bond angles with their estimated standard deviations are listed in Table 2.

Table 1
Crystal data and structure refinement information for complex **1**.

Empirical formula	$C_{60}H_{76}Cl_2N_8O_{18}Zn_5$
Formula weight	3190.28
Crystal system	Monoclinic
Space group	$P2_1/c$
a, Å	11.2589 (16)
b, Å	12.957 (2)
c, Å	24.206 (4)
β, deg	102.403 (3)
V, Å^3	3448.8 (9)
Z	2
μ, mm^{-1}	1.864
Reflections collected	18 248
Unique reflections	6755
Obs. reflections [$I > 2\sigma(I)$]	5820
R_{int}	0.029
R_1 [$I > 2\sigma(I)$]	0.0465
wR_2 [$I > 2\sigma(I)$]	0.1172
Goodness-of-fit	1.03

Table 2
Selected bond lengths (Å) and bond angles (degrees) for Complex **1**.

Zn1–O1	1.996 (2)	Zn1–N1A	2.184 (3)	Zn1–N2A	2.088 (3)
Zn1–N3A	2.070 (3)	Zn1–N4A	2.104 (3)	Zn2–Cl1	2.3010 (10)
Zn2–O2	2.096 (2)	Zn2–O3	2.367 (3)	Zn2–O4B	1.983 (2)
Zn2–O6C	2.038 (3)	Zn2–O7C	2.453 (3)	Zn3–O3	2.173 (3)
Zn3–O7F	2.133 (3)	Zn3–O5B	2.018 (2)	Zn3–O3D	2.173 (3)
Zn3–O7C	2.133 (3)	Zn3–O5E	2.018 (2)		
N1A–Zn1–N2A	83.35 (10)	N1A–Zn1–N4A	82.26 (11)	N1A–Zn1–N3A	83.22 (11)
O1–Zn1–N1A	172.60 (10)	O2–Zn2–O3	167.03 (9)	O4B–Zn2–O6C	148.11 (11)
Cl1–Zn2–O7C	160.08 (7)	O3–Zn3–O3D	180.00	O7F–Zn3–O7C	180.00
O5B–Zn3–O5E	180.00	O5B–Zn3–O7F	89.68 (9)	O3D–Zn3–O5B	89.29 (9)
O3D–Zn3–O7C	97.16 (10)	O3–Zn3–O7C	82.85 (10)	O5E–Zn3–O7F	90.32 (9)

Symmetry codes. $A = -x, -1/2+y, 1/2-z$; $B = 1-x, -1/2+y, 1/2-z$; $C = -x, 1-y, 1-z$; $D = -x, -y, 1-z$; $E = -1+x, 1/2-y, 1/2+z$; $F = x, -1+y, z$.x

3. Results and discussion

3.1. Crystal structures of $[Zn_5(trencba)_2(OH)_2Cl_2 \cdot 4H_2O]$ (**1**)

As shown in Fig. 1a, there are three crystallographically independent Zn atoms in the asymmetry unit: Zn(1) is pentahedrally coordinated to four amide N atoms in trigonal prismatic arrangement and one carboxylate oxygen atom; Zn2 is octahedrally bound to four carboxylate oxygen atoms from three different ligands, one μ_2-OH group as well as one Cl anion ion; the occupancy for Zn3 is 0.5, which is also in octahedron, composed by two μ_2-OH moieties and four carboxylate oxygen atoms from four discrete ligands. The average Zn–O and Zn–N distances are 2.129 and 2.112 Å, respectively, which compares well with the distance found in other zinc(II) structures [23]. Obviously, the bond lengths of Zn2–O3 and Zn2–O7C are longer than other Zn–O distances (Scheme 1).

As illustrated in Fig. 1a, **1** is constructed from a penta-nuclear zinc cluster fragment. Carboxylate groups from six different ligands, eight nitrogen from two distinct ligands and two μ_2-OH connect five zinc atoms arranged linearly to form a penta-nuclear fragment. No such fragment has been reported prior to this work. It should be noted that Zn3 are sited at the inversion center in the fragment. Each μ_2-OH anion bridges Zn2 and Zn3 ions, with the Zn2···Zn3 distances and an angle of 3.422 Å and 97.72(10)°, respectively, which is similar to that found in the literature [24,25]. Moreover, Zn1 and Zn2 atoms are connected only by one carboxylate group with the separation of 4.628 Å.

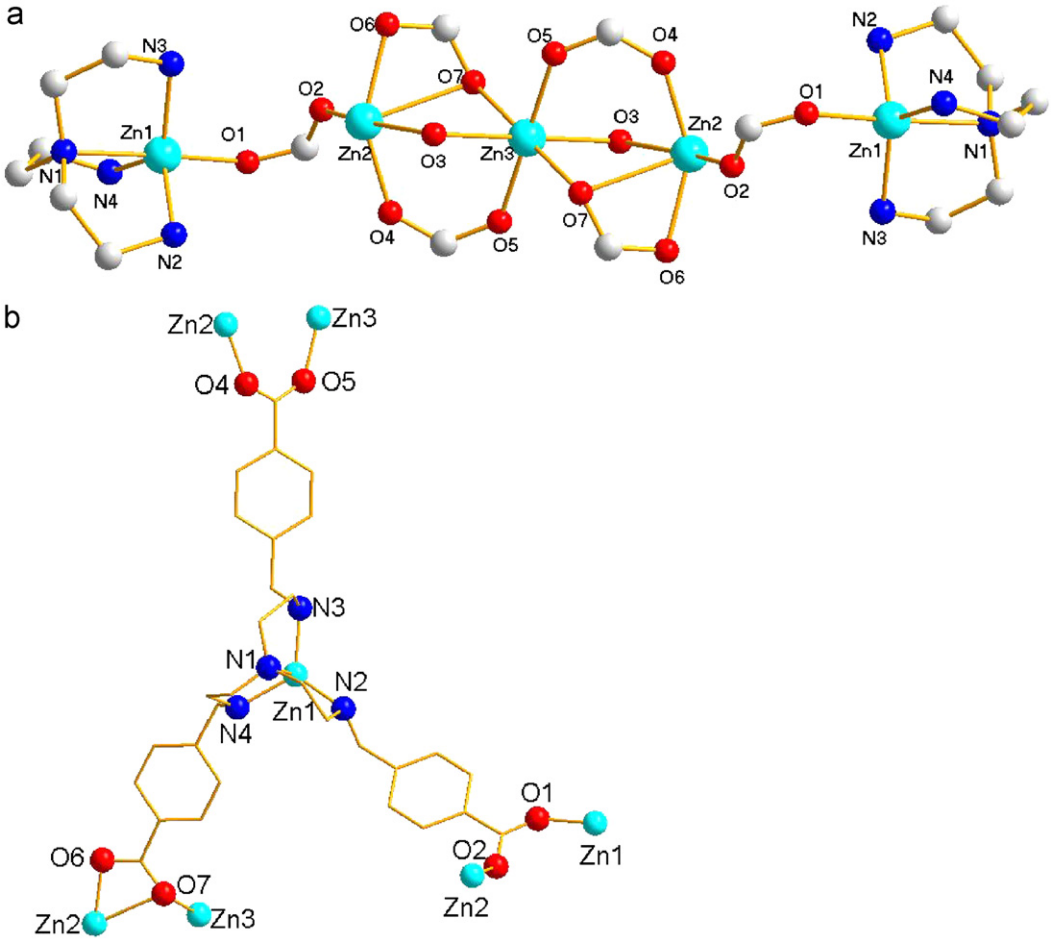

Fig. 1. (a) The unprecedented penta-nuclear fragment in complex **1**. (b) The coordination mode of trencba^{3-} in complex **1**.

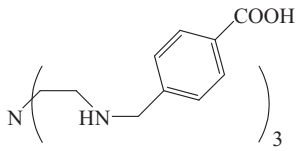

Scheme 1. H_3trencba.

Ligands H_3trencba are coordinated to Zn ions in the mode as displayed in Fig. 1b. In each ligand, two carboxylate groups adopt bidentate bridging modes, respectively, linking two zinc atoms; meanwhile, the remaining carboxylate with a chelating-bridging mode also connects two zinc atoms, and thus the ligand acting as a μ_6 bridging ligand links four penta-nuclear zinc cluster fragments, and every fragment connects eight ligands to generate a three-dimensional non-interpenetrated porous framework, as shown in Fig. 2a and b. In fact, the uncoordinated water molecules are trapped in the voids, which constitute 17.7% of the unit cell volume [26]. As anticipated, the lattice water O8W is involved in hydrogen-bond interactions with free water O1W and ClG with separation of 2.756(5) and 3.287(3) Å, respectively; moreover, the hydroxyl group O3 forms stronger hydrogen bond with the lattice water O8WI with distance of 2.746(4) Å. Furthermore, the C23 atom also has weak interaction with carboxylate groups O1J, C23–H23···O1J distance of 3.041(4) Å (Table S1). The extensive hydrogen bonds may contribute for the stability of the structure.

For better insight into the intricate polymeric framework of compound **1**, topological analysis is completed. If Zn3 atoms are used to represent the Zn2 and Zn3 tri-cluster unit, Zn1 atom can be simply considered as a node linking four Zn3 and two Zn1 atoms whereas Zn3 atom acts as the other node connecting eight Zn1 atoms. As a result, compound **1** exhibits a rare (6,8)-connected 3D bi-nodal topology, which can be described by the Schläfli symbol of $(3^4 4^7 5^4)_2(3^4 4^8 5^4 6^8 7^4)$ with the vertex symbols for the 6-connected Zn1 nodes and 8-connected Zn3 nodes, as illustrated in Fig. 3. This is the first example of (6,8)-connected 3D bi-nodal framework based on a single kind of organic ligand.

3.2. IR spectra

A broad peak at 3406 cm^{-1} observed in complex **1** suggests lattice water molecule in existence. The absence of 1715 cm^{-1} indicates all carboxylates are completely deprotonated. The unidentate carboxylate group shows a very strong broad ν_{asym} stretching at 1592 cm^{-1} and the corresponding ν_{sym}(COO) were observed at 1407, 1385 cm^{-1}, with $\Delta\nu$ value of 185–207 cm^{-1}. As anticipated, the bidentate chelate carboxylate moiety exhibits ν_{asym}(COO) at a lower frequency at 1545 and 1528 cm^{-1}, with $\Delta\nu$ value of 138–143 cm^{-1} [27].

3.3. TG and XRD

Complex **1** is stable at ambient conditions, and thermogravimetric experiment was performed to explore thermal stabilities. For **1**, the first weight loss occurs in the range of 96 to 140 °C,

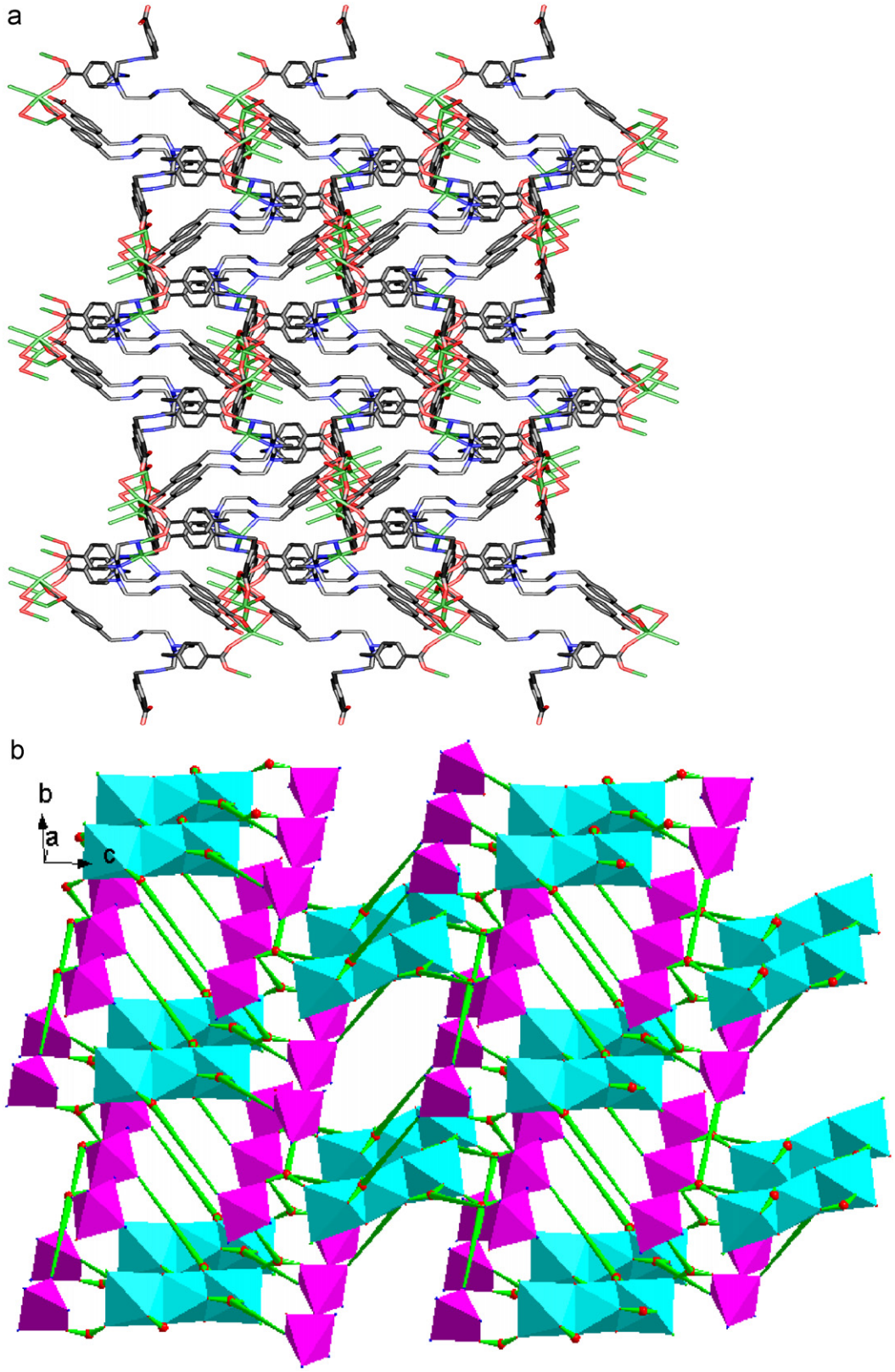

Fig. 2. (a) 3D packing diagram of **1** on the *bc* plane with open channels. (b) Simplified scheme of **1** (purple polyhedron represents Zn1 coordination environment and blue polyhedron represents Zn2 and Zn3 tri-cluster unit).

which is attributed to the departure of the lattice water molecules (obsd 4.43%, calcd 4.50%), followed by a plateau region ranging from 140 to 290 °C. The second weight loss occurs in the range 290 and 398 °C, which results from the elimination of the tren moiety (obsd 23.95%, calcd 23.52%). The third weight loss occurs in the range 398 and 441 °C corresponding to the burning of one benzene ring molecule (obsd 12.85%, calcd 12.83%). The fourth weight loss occurs in the range 441 and 506 °C, corresponding to

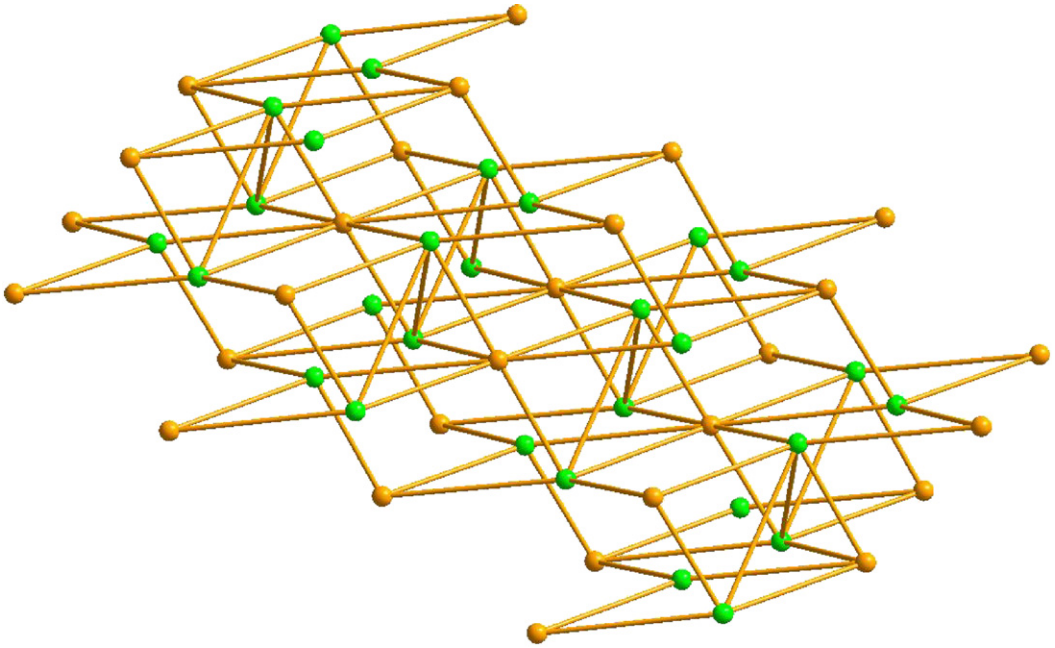

Fig. 3. The (6,8)-connected topological network for compound **1** (green atoms indicate 6-connected atoms Zn1, and yellow atoms suggest 8-connected atoms Zn3).

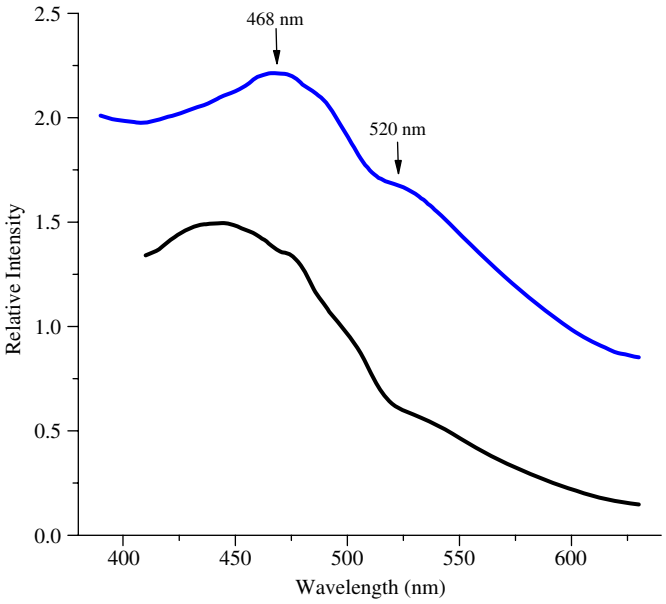

Fig. 4. Fluorescent emission spectra of complex **1** (upper) and free ligand (lower) in solid state at room temperature.

the departure of μ_2-OH and Cl moieties (obsd 8.75%, calcd 8.63%) and consecutive decompositions suggest the total destruction of the framework.

The purity of complex **1** was confirmed by X-ray power diffraction analyses, in which the experimental spectrum of the compound is almost consistent with its simulated spectrum (Fig. S3).

3.4. Photoluminescence properties

The emission spectra of complex **1** and free ligand in the solid state at room temperature were investigated, as depicted in Fig. 4. Upon excitation at *ca.* 325 nm, complex **1** exhibits blue fluorescent emission bands at *ca.* 468 and 520 nm, which can probably be assigned to the intraligand ($\pi-\pi^*$) fluorescent emission because similar weaker emissions are observed for the free H_3trencba·HCl. The enhancement of the emissions for **1** compared with those of the free ligand may be ascribed to the increase in the ligand conformational rigidity due to their coordination to Zn(II) ions resulting in a decrease in the nonradiative decay of intraligand excited states [28,29]. The complex may be used as a potential material for blue-light-emitting diode devices.

4. Conclusions

In this paper, we report the synthesis and characterizations of a novel 3D porous MOF, $[Zn_5(trencba)_2(OH)_2Cl_2\cdot 4H_2O]$, with unprecedented penta-nuclear zinc cluster fragment, which is constructed from a flexible divergent bi-functional ligand. Compound **1** is the first example of (6,8)-connected 3D bi-nodal framework based on a single kind of organic ligand. Moreover, complex **1** displays relatively stronger blue emissions at room temperature than that of the ligand, therefore, it appears to be a good candidate of hybrid inorganic–organic photo-active materials. In summary, our research demonstrates that the H_3trencba ligand could be a potential building block with the combination of transition metal ions to construct novel supramolecular architecture with unusual topology and property.

Supplementary material

Crystallographic data for the structure reported in this paper have been deposited with the Cambridge Crystallographic Data Centre as supplementary publication no. CCDC_689994. Copies of the data can be obtained free of charge on application to CCDC, 12 Union Road, Cambridge CB2 1EZ, UK (fax: (44) 1223 336-033; e-mail: deposit@ccdc.cam.ac.uk).

Acknowledgments

This work was financially supported by the National Nature Science Foundation of China (Nos. 20801021 and 20802022) and the Program for Chenguang Young Scientists of Wuhan (200850731361).

Appendix A. Supplementary data

Supplementary data associated with this article can be found in the online version at 10.1016/j.jssc.2008.11.031.

References

[1] J.M. Lehn, Supramolecular Chemistry: Concepts and Perspectives, VCH, New York, 1995.
[2] G.R. Desiraju, Crystal Design: Structure and Function, Perspectives in Supramolecular Chemistry, vol. 6, Wiley, Chichester, 2003.
[3] M. Eddaoudi, D.B. Moler, H.L. Li, B.L. Chen, T.M. Reineke, M. O'Keeffe, O.M. Yaghi, Acc. Chem. Res. 34 (2001) 319.
[4] S.L. James, Chem. Soc. Rev. 32 (2003) 276.
[5] A.N. Khlobystov, A.J. Blake, N.R. Champness, D.A. Lemenovskii, A.G. Majouga, N.V. Zyk, M. Schröder, Coord. Chem. Rev. 222 (2001) 155.
[6] Y.Q. Lan, X.L. Wang, S.L. Li, Z.M. Su, K.Z. Shao, E.B. Wang, Chem. Commun. (2007) 4863.
[7] N.L. Rosi, J. Eckert, M. Eddaoudi, D.T. Vodak, J. Kim, M. O'Keeffe, O.M. Yaghi, Science (2003) 1127.
[8] A.C. Sudik, A.P. Côté, O.M. Yaghi, Inorg. Chem. 44 (2005) 2998.
[9] A.C. Sudik, A.P. Côté, A.G. Wong-Foy, M. O'Keeffe, O.M. Yaghi, Angew. Chem. Int. Ed. 45 (2006) 2528.
[10] S.S. Kaye, A. Dailly, O.M. Yaghi, J.R. Long, J. Am. Chem. Soc. 129 (2007) 14176.
[11] S.Q. Ma, H.C. Zhou, J. Am. Chem. Soc. 128 (2006) 11734.
[12] D.F. Sun, S.Q. Ma, Y.X. Ke, D.J. Collins, H.C. Zhou, J. Am. Chem. Soc. 128 (2006) 3896.
[13] S.Q. Ma, X.S. Wang, C.D. Collier, E.S. Manis, H.C. Zhou, Inorg. Chem. 46 (2007) 8499.
[14] S. Neogi, J.A.R. Navarro, P.K. Bharadwaj, Cryst. Growth Des. 8 (2008) 1554.
[15] S. Neogi, G. Savitha, S. Neogi, Inorg. Chem. 43 (2004) 3771.
[16] S. Neogi, P.K. Bharadwaj, Cryst. Growth Des. 6 (2006) 433.
[17] S.N. Wang, H. Xing, Y.Z. Li, J.F. Bai, M. Scheer, Y. Pan, X.Z. You, Chem. Commun. (2007) 2293.
[18] S.N. Wang, J.F. Bai, Y.Z. Li, Y. Pan, M. Scheerb, X.Z. You, Cryst. Eng. Commun. 9 (2007) 1084.
[19] H.F. Zhu, J. Fan, T.-A. Okamura, Z.H. Zhang, G.X. Liu, K.B. Yu, W.Y. Sun, N. Ueyama, Inorg. Chem. 45 (2006) 3941.
[20] Z.H. Zhang, Z.L. Shen, T.-A. Okamura, H.F. Zhu, W.Y. Sun, N. Ueyama, Cryst. Growth Des. 5 (2005) 1191.
[21] SMART and SAINT, Area Detector Control and Integration Software; Siemens Analytical X-ray Systems, Inc., Madison, WI, 1996.
[22] G.M. Sheldrick, SHELXTL V5.1, Software Reference Manual; Bruker AXS, Inc., Madison, WI, 1997.
[23] S. Neogi, P.K. Bharadwaj, Inorg. Chem. 44 (2005) 816.
[24] L.L. Wen, Y.Z. Li, Z.D. Lu, J.G. Lin, C.Y. Duan, Q.J. Meng, Cryst. Growth Des. 6 (2006) 530.
[25] Z. Shi, G.H. Li, L. Wang, L. Gao, X.B. Chen, J. Hua, S.H. Feng, Cryst. Growth Des. 4 (2004) 25.
[26] A.L. Spek, PLATON, A Multipurpose Crystallographic Tool, Utrecht University, Utrecht, The Netherlands, 1999.
[27] G.B. Deacon, R.J. Phillips, Coord. Chem. Rev. 33 (1980) 227.
[28] A.W. Adamson, P.D. Fleischauer, Concepts of Inorganic Photochemistry, Wiley, New York, 1975.
[29] H. Yersin, A. Vogler (Eds.), Photochemistry and Photophysics of Coordination Compounds, Springer, Berlin, 1987.